Available online at www.sciencedirect.com
ScienceDirect
Journal of Sound and Vibration 302 (2007) 716–727
JOURNAL OF SOUND AND VIBRATION
www.elsevier.com/locate/jsvi

Low-frequency vibration control of a pan/tilt platform with vision feedback

Yin-Chieh Chang, Jinsiang Shaw*

Institute of Mechatronic Engineering, National Taipei University of Technology, No. 1, Sec. 3, Zhongxiao E. Road, Taipei 106, Taiwan, ROC

Received 26 August 2005; received in revised form 24 April 2006; accepted 4 December 2006
Available online 20 February 2007

Abstract

This paper aims to develop active control techniques with vision feedback for suppressing low-frequency vibration of a device mounted on a pan/tilt platform due to its base disturbances. Pan/tilt platforms are commonly seen in the head of a waking robot, in an antenna, in a vision surveillance equipment, in a cannon platform, etc., for yaw and pitch direction control. However, due to its inevitable low-frequency base vibration possibly from road or sea wave disturbance in a mobile situation, orientation control of the device mounted on the top tilt platform can be seriously affected. In this paper, an adaptive sliding control (ASC) scheme is first derived and employed for vibration attenuation. Function approximation technique is used to represent the unknown disturbance in some finite linear combination of the orthogonal basis. The dynamics of pan/tilt system can thus be proved to be a stable first-order filter driven by function approximation errors. Moreover, the adaptive update law can be obtained by using the Lyapunov stability theory. Secondly, the frequently used feedback active vibration control (AVC) with filtered-x LMS algorithm is to be used and compared with the adaptive sliding control for vibration suppression performance. Experimental tests of the control algorithms show that for independent single axis excitation, about 25.14 and 23 dB attenuations in average for single-frequency disturbance have been obtained by using the ASC and feedback AVC, respectively. For dual-frequency excitation, the vibration attenuations are about 20.77 and 12.73 dB by the two methods, respectively. As for simultaneous two axes excitations, ASC and feedback AVC have respective 17.57 and 15.18 dB vibration reductions under single-frequency disturbances. Thus, validity and effectiveness of the two active control methods with vision feedback for suppressing low-frequency vibration of the device on the pan/tilt platform is verified.

1. Introduction

Owing to rapid development of hardware and personal computers in recent years, PC-based real-time vision feedback control becomes a viable option for many applications, such as auto pilot vehicle and mobile robot [1], etc. The sequence of image always contains a lot of information. Thus, visual feedback technique is applicable to many well-known problems, for example, the inverted pendulum [2] and ball-beam balancing systems [3].

*Corresponding author.
E-mail address: jshaw@ntut.edu.tw (J. Shaw).

0022-460X/$ - see front matter © 2007 Elsevier Ltd. All rights reserved.
doi:10.1016/j.jsv.2006.12.025

Vision feedback system is one that combines vision as an integral part of system loop. In earlier stage, some simple compensators such as PID were applied to stabilize and improve performance for vision feedback system [4]. Use of PID controller may work for some systems. However, most visual servo systems have the problem of varying time-delay. The delays depend on the amount of image processing required. Constant time delays may come from optical flow algorithm, etc. Some other image processing algorithms, for example pattern recognition, edge detection, or feature detection, will have a varying time delay between frame to frame. These time delays depend on the number of features obtained. In general, relative stability and system performance degrade when time delay exists. Using frequency response method, we can easily obtain that the phase margin decreases as time delay getting larger. Thus, ignoring this effect may lead the system to instability.

Recently, the approach of linear regulator (LQG) has been applied in vision feedback system [5]. This approach has ability to minimize the noise from sensor. Nevertheless, the optimal performance is difficult to achieve. To acquire better performance, careful selection of the weighting matrices is necessary. In most situations, weighting matrices can only be obtained by trial-and-error method to complete controller design. Furthermore, this approach can tolerate only small modeling error. One important modeling error is the uncertainty between actual focal distance and nominal one. Therefore, system should be modeled exactly to avoid instability. This problem can be overcome by using self-tuning adaptive controller (STAC) [6,7]. This control scheme attempts to estimate on line the uncertain parameters and adjust the gains accordingly. Hence, STAC gives good modeling errors and delay toleration. Although this method has ability to address the effect of modeling uncertainties and delays, the stability is not easy to prove. Indeed, the stability and convergence of STACs are generally quite difficult to guarantee, often requiring the signals in the system to satisfying persistent excitation (PE) condition so that the estimate parameters converge to real parameters. On the other hand, the stability and convergence may not be guaranteed while the reference signals are not very rich [8].

The robust control scheme can be applied in this stage to improve the performance and stability of vision servo system. There are some well-known robust control laws, such as H_∞, Lyapunov redesign, and sliding control, etc. In this research, an adaptive sliding controller and function approximation technique are proposed to deal with modeling uncertainty and unknown disturbance [9–14]. Sliding control is an effective approach of robust control laws [8]. It could effectively conquer the effects from modeling imprecision, such as neglected time-delay, inaccuracies on the gain constant of actuators, friction, and so on. The direction of control action is determined by sliding condition to force the system evolving on the sliding surface. Moreover, the behavior of system is like a low-pass filter. The uncertainties should be defined in a compact set while using this approach. However, the variation bound of uncertainties may not easily be obtained. Therefore, the traditional robust or adaptive controller may not be used directly when the variation bounds are not given. Since the uncertainties are assumed to be time varying, function approximation technique may be used here to represent the unknown disturbances or uncertainties in some finite linear combinations of the orthogonal basis functions. Moreover, the update law of coefficients of approximation series can be obtained by using Lyapunov-like design. The system convergence can thus be proved for all bounded reference signal inputs.

In this paper, a pan/tilt platform with two degrees of freedom is used for studying vibration suppression of the developed adaptive sliding controller with vision feedback. Performance of the adaptive sliding controller for suppressing vibrations of a device mounted on such a pan/tilt platform due to its base disturbances is to be compared with that using another well-unknown algorithm of feedback AVC.

2. Problem description

A pan/tilt platform for study of yaw and pitch vibration control is constructed as shown in Fig. 1. The upper tilt table is mounted on the pan platform, both platforms being controlled by respective motors via transmission belts. Two RVDT sensors are employed for measuring respective yaw and pitch angles relative to the base and the pan table, respectively. These yaw and pitch angles are to be used for stabilizing respective platforms. The base of the constructed pan/tilt platform is attached to a Steward platform [15], which can provide desired disturbance waveforms to the pan/tilt platform, simulating any realistic low-frequency excitation to the platform. A CCD camera is mounted on top tilt platform for vision feedback of the

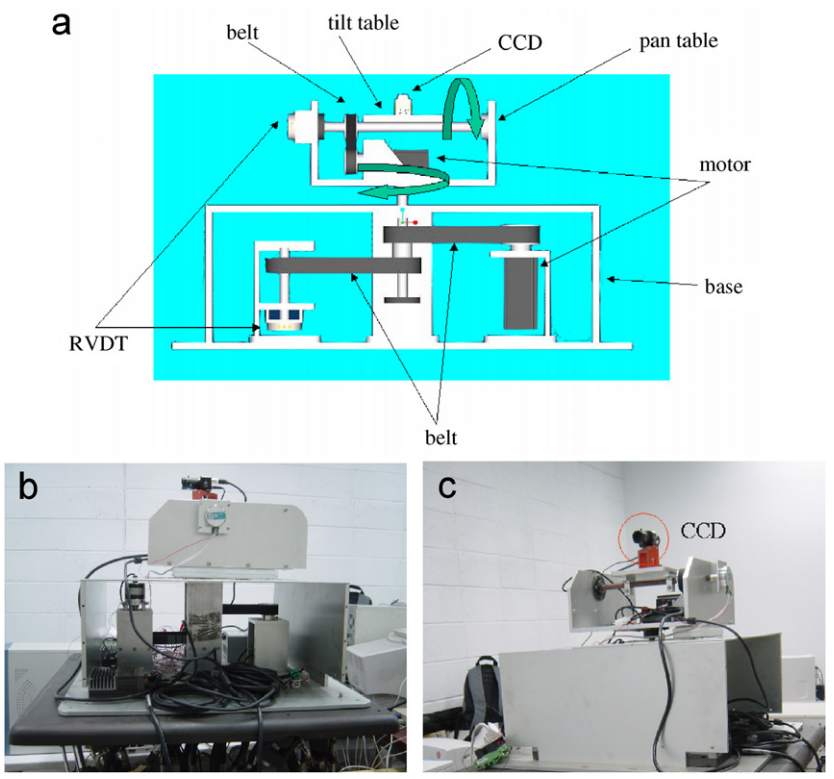

Fig. 1. Pan/tilt platform with a CCD camera attached atop: (a) platform layout, (b) lateral view of constructed platform, (c) front view of constructed platform.

coordinates of a target. By appropriately controlling servo motors in both the pan and base platforms, the target can be hold steady at the origin of the image plane despite of base vibrations, namely a locked target by the CCD camera is obtained in spite of persistent base excitations. Due to its decoupled structure, the dynamic equations in yaw and pitch direction can simply be derived as Eq. (1)

$$\begin{cases} \dot{x}_1 = x_2, \\ \dot{x}_2 = \dfrac{1}{I_1} T_1 + d_1(t), \\ \dot{x}_3 = x_4, \\ \dot{x}_4 = \dfrac{1}{I_2} T_2 + d_2(t), \end{cases} \tag{1}$$

where $x_i \in \Re$, $i = 1,\ldots,4$ are state variables, and the output $y = \begin{bmatrix} x_1 & x_3 \end{bmatrix}^{\mathrm{T}}$ is the angular displacement vector of pan/tilt platform in yaw and pitch directions. The inertia of platform I_k, $k = 1,\ldots,2$ are positive values and $d_k(t)$ are the time-varying disturbances from the Steward platform. T_k are the control torque inputs from servo motors. A reasonable assumption in this experiment is that I_k are unknown positive constants, and that $d_k(t)$ are bounded unknown disturbances; moreover, the variation bounds are not available. The control issue is to design a controller for disturbance rejection so that a flat and quiescent tilt platform can be maintained. However, the bound of $d_k(t)$ are not available. Therefore, traditional robust control scheme cannot be used directly in this stage. Since the parameter and disturbance bound are unknown, the adaptive algorithm could be used to solve these problems. In the paper, two control methods of adaptive sliding control with function approximation technique and feedback AVC using linear adaptive filter are applied to deal with above problems.

3. Theoretic background

3.1. Image processing algorithm

Fig. 2 illustrates the vision system used for image feedback. A model of the image formation process is shown in Fig. 2(a). We define the camera coordinate system (x, y, z) as having the image plane coincident with the xy plane, and optical axis (established by the center of the lens) along the z-axis. Thus, the center of the image plane is at the origin, and the center of the lens is at coordinates $(0, 0, \lambda)$. If the camera is in focus for distant objects, λ is the focal length of lens. In this section, it is assumed that the camera coordinate system is aligned with the world coordinate system $(X–Z)$. P and P_1 denote the target point and its projection on the image plane, respectively. Fig. 2(b) shows the relationship between CCD and target point P. The control objective is to keep point P_1 in the center of the image plane under base excitations. For small tilt angular displacement, the focus length λ is assumed to be constant. By the position of P_1 in the image plane, we may calculate the angular displaces of respective pan and tilt platforms.

The projected position x_1 and y_1 of target P in the image plane can be obtained by calculating the centroid [16], as shown in Eq. (2):

$$x_1 = \frac{m_{10}}{m_{00}}, \quad y_1 = \frac{m_{01}}{m_{00}}, \tag{2}$$

where m_{01}, m_{10} and m_{00} are the moment of the target, which can be calculated by Eq. (3):

$$m_{pq} = \int_{-\infty}^{\infty} x^p y^q f(x, y)\,\mathrm{d}x\,\mathrm{d}y. \tag{3}$$

$f(x, y)$ denotes the gray level value at pixel (x, y). The gray level of $f(x, y)$ at this stage takes on either 255 when it is part of the target or 0 otherwise after using two simple digital image processing algorithms, namely thresholding and negating the image. The discrete form of Eq. (3) is derived as in Eq. (4), where m and n are the size of the image:

$$m_{pq} = \sum_{x=1}^{m}\sum_{y=1}^{n} x^p y^q f(x, y). \tag{4}$$

Therefore, we can obtain the pitch and yaw angles as

$$\theta_{\text{pitch}} \approx \tan^{-1}\frac{y_1}{\lambda}, \quad \theta_{\text{yaw}} \approx \tan^{-1}\frac{x_1}{\lambda}. \tag{5}$$

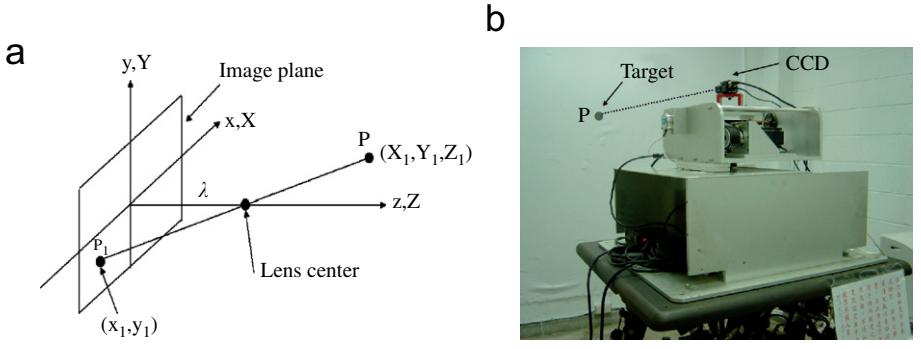

Fig. 2. Vision system for image feedback: (a) camera coordinate system, (b) relationship between CCD and target.

3.2. Adaptive sliding controller design

In this section, design procedures of adaptive sliding controller for pan/tilt platform are briefly given. First we define sliding surfaces s_1 and s_2 as

$$\begin{cases} s_1 = \left(\dfrac{\mathrm{d}}{\mathrm{d}t} + \lambda_1\right)\tilde{x}_1 = \tilde{x}_2 + \lambda_1\tilde{x}_1, \\ s_2 = \left(\dfrac{\mathrm{d}}{\mathrm{d}t} + \lambda_2\right)\tilde{x}_3 = \tilde{x}_4 + \lambda_2\tilde{x}_3, \end{cases} \tag{6}$$

where $\tilde{x}_i = x_i - x_{id}$, $i = 1, 2, 3, 4$ and λ_k is a parameter to be arbitrarily selected to give proper bandwidth for the system when evolving on the sliding surface. Note that x_{id} is the desired value of respective x_i. By taking time derivative in Eq. (6), we can obtain

$$\begin{cases} \dot{s}_1 = \dot{x}_2 - \dot{x}_{2d} + \lambda_1\tilde{x}_2 = m_1u_1 + d_1 - \dot{x}_{2d} + \lambda_1\tilde{x}_2, \\ \dot{s}_2 = \dot{x}_4 - \dot{x}_{4d} + \lambda_2\tilde{x}_4 = m_2u_2 + d_2 - \dot{x}_{4d} + \lambda_2\tilde{x}_4, \end{cases} \tag{7}$$

where $m_k = 1/I_k$ and $u_k = T_k$. Eq. (7) can also be represented as

$$\begin{cases} \dot{s}_1 = (m_1 - \hat{m}_1)u_1 + \hat{m}_1u_1 + d_1 - \dot{x}_{2d} + \lambda_1\tilde{x}_2, \\ \dot{s}_2 = (m_2 - \hat{m}_2)u_2 + \hat{m}_2u_2 + d_2 - \dot{x}_{4d} + \lambda_2\tilde{x}_4. \end{cases} \tag{8}$$

We may select the following u_k to stabilize the system

$$\begin{cases} u_1 = \dfrac{1}{\hat{m}_1}\left[-\hat{d}_1 + \dot{x}_{2d} - \lambda_1\tilde{x}_2 - \eta_1\left(\dfrac{s_1}{\phi_1}\right)\right], \\ u_2 = \dfrac{1}{\hat{m}_2}\left[-\hat{d}_2 + \dot{x}_{4d} - \lambda_2\tilde{x}_4 - \eta_2\left(\dfrac{s_2}{\phi_2}\right)\right] \end{cases} \tag{9}$$

and Eq. (8) becomes

$$\begin{cases} \dot{s}_1 = (m_1 - \hat{m}_1)u_1 + (d_1 - \hat{d}_1) - \eta_1\left(\dfrac{s_1}{\phi_1}\right), \\ \dot{s}_2 = (m_2 - \hat{m}_2)u_2 + (d_2 - \hat{d}_2) - \eta_2\left(\dfrac{s_2}{\phi_2}\right), \end{cases} \tag{10}$$

where $\hat{m}_k$ and $\hat{d}_k$ are the estimate values of m_k and d_k, respectively. The positive values η_k are to be determined. ϕ_k is the respective width of the sliding boundary layer. Assume that functions d_k and $\hat{d}_k$ satisfy the Dirichlet's condition. Therefore, they can be each represented by a linear combination of the orthonormal basis $\{z_j(t)\}$, $j = 1, \ldots,$

$$\begin{aligned} d_k(t) &= \sum_{j=1}^{n} w_{kj}z_j(t) + \sum_{j=n+1}^{\infty} w_{kj}z_j(t), \\ \hat{d}_k(t) &= \sum_{j=1}^{n} \hat{w}_{kj}z_j(t), \end{aligned} \qquad k = 1, 2. \tag{11}$$

We would like to abuse the notation by writing the approximation as

$$\begin{aligned} d_k(t) &= w_k^{\mathrm{T}}z + \varepsilon_k, \\ \hat{d}_k(t) &= \hat{w}_k^{\mathrm{T}}z, \end{aligned} \tag{12}$$

where w, $\hat{w} \in \Re^n$ are weighting vectors, $z \in \Re^n$ is the vector of basis function, the positive constant n is the number of basis functions used in the approximation, ε_k is the truncation error. Then, Eq. (10) can be

rewritten as

$$\dot{s}_k = \tilde{m}_k u_k + \tilde{w}_k^{\mathrm{T}} z - \eta_k \left(\frac{s_k}{\phi_k}\right) + \varepsilon_k, \quad k = 1, 2, \tag{13}$$

where $\tilde{w}_k = w_k - \hat{w}_k$ and $\tilde{m}_k = m_k - \hat{m}_k$ are the corresponding estimate errors. The dynamics of pan/tilt system are thus proved to be stable first order filters driven by function approximation errors. The update laws of the basis coefficients $\hat{w}_k$ and constant $\hat{m}_k$ can be derived by applying the Lyapunov stability theory. Let us define Lyapunov function candidates as

$$V_k = \tfrac{1}{2} s_k^2 + \tfrac{1}{2} \tilde{w}_k^{\mathrm{T}} Q_k \tilde{w}_k + \tfrac{1}{2} \rho_k \tilde{m}_k^2 > 0, \quad k = 1, 2, \tag{14}$$

where Q_k is a positive definite matrix and ρ_k is a positive value. Taking time derivative of Eq. (14) yields

$$\dot{V}_k = s_k \left(\tilde{m}_k u_k + \tilde{w}_k^{\mathrm{T}} z - \eta_k \frac{s_k}{\phi_k} + \varepsilon_k\right) - \tilde{w}_k^{\mathrm{T}} Q_k \dot{\hat{w}} - \rho_k \tilde{m}_k \dot{\hat{m}}_k. \tag{15}$$

Therefore, the update law can be chosen as

$$\dot{\hat{m}}_k = \rho_k^{-1} s_k u_k, \tag{16}$$

$$\dot{\hat{w}}_k = Q_k^{-1} z s_k. \tag{17}$$

However, Eq. (16) can be further modified to avoid the singularity problem

$$\dot{\hat{m}}_k = \begin{cases} \rho_k^{-1} s_k u_k & \text{if } \hat{m}_k > \underline{m_k}, \\ \rho_k^{-1} s_k u_k & \text{if } \hat{m}_k = \underline{m_k} \quad \text{and } s_k u_k > 0, \\ 0 & \text{if } \hat{m}_k = \underline{m_k} \quad \text{and } s_k u_k \leqslant 0, \end{cases} \tag{18}$$

where $\underline{m_k}$ is a known lower bound of m_k. By substituting Eqs. (17) and (18) into Eq. (15), we can obtain

$$\dot{V}_k = \left(-\eta_k \frac{|s_k|}{\phi_k} + |\varepsilon_k|\right)|s_k|. \tag{19}$$

If sufficient number of basis functions are used such that function approximation error $\varepsilon_k \approx 0$, then Eq. (19) becomes

$$\dot{V}_k = \left(-\eta_k \frac{s_k^2}{\phi_k}\right) \leqslant 0. \tag{20}$$

From Eq. (20), we can easily find that the system is uniformly stable and s_k, $\tilde{m}_k$, $\tilde{w}_k \in L_\infty$. By Eq. (13) we can have $\dot{s}_k \in L_\infty$. To acquire the asymptotical stable, we need to prove that $s_k \in L_2$. It can be proved by Eq. (21)

$$\int_0^\infty s_k^2 \, \mathrm{d}t = -\frac{\phi_k}{\eta_k} \int_0^\infty \dot{V}_k \, \mathrm{d}t = -\frac{\phi_k}{\eta_k} (V_{k\infty} - V_{k0}) < \infty. \tag{21}$$

Since $s_k \in L_\infty \cap L_2$ and $\dot{s}_k \in L_\infty$, by Barbalat's lemma we can have asymptotical stability of the system. In addition, since $\tilde{m}_k$, $\tilde{w}_k \in L_\infty$, all estimations therefore remain bounded.

Remark 1. If approximation error cannot be neglected, and there exists a positive constant $\delta_k > 0$ such that $|\varepsilon_k| \leqslant \delta_k$. To tackle this bounded approximation error, Eq. (9) can be modified to be

$$\begin{cases} u_1 = \dfrac{1}{\hat{m}_1}\left[-\hat{d}_1 + \dot{x}_{2d} - \lambda_1 \tilde{x}_2 - \eta_1 \left(\dfrac{s_1}{\phi_1}\right)\right] + u_{\text{robust\_1}}, \\ u_2 = \dfrac{1}{\hat{m}_2}\left[-\hat{d}_2 + \dot{x}_{4d} - \lambda_2 \tilde{x}_4 - \eta_2 \left(\dfrac{s_2}{\phi_2}\right)\right] + u_{\text{robust\_2}}. \end{cases} \tag{22}$$

Then, we have

$$\dot{V}_k = \left(-\eta_k \frac{s_k^2}{\phi_k}\right) + |s_k||\varepsilon_k| + s_k u_{\text{robust\_}k}. \tag{23}$$

By selecting $u_{\text{robust\_}k} = -\text{sgn}(s_k)\delta_k$, we still can have asymptotical stability of the system.

Remark 2. To avoid parameter drift, the σ modification technique [17] can be used to Eqs. (17) and (18):

$$\dot{\hat{w}}_k = Q_k^{-1} z s_k - \sigma_w \hat{w}, \tag{24}$$

$$\dot{\hat{m}}_k = \begin{cases} \rho_k^{-1} s_k u_k - \sigma_m \hat{m} & \text{if } \hat{m}_k > \underline{m_k}, \\ \rho_k^{-1} s_k u_k - \sigma_m \hat{m} & \text{if } \hat{m}_k = \underline{m_k} \quad \text{and } s_k u_k > 0, \\ 0 & \text{if } \hat{m}_k = \underline{m_k} \quad \text{and } s_k u_k \leqslant 0, \end{cases} \tag{25}$$

where σ_w and σ_m are small positive constants.

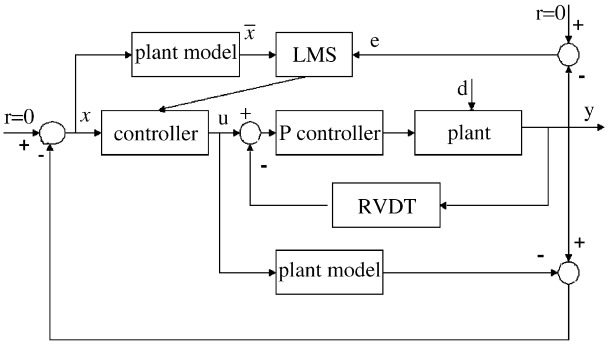

Fig. 3. Block diagram of a feedback active vibration control.

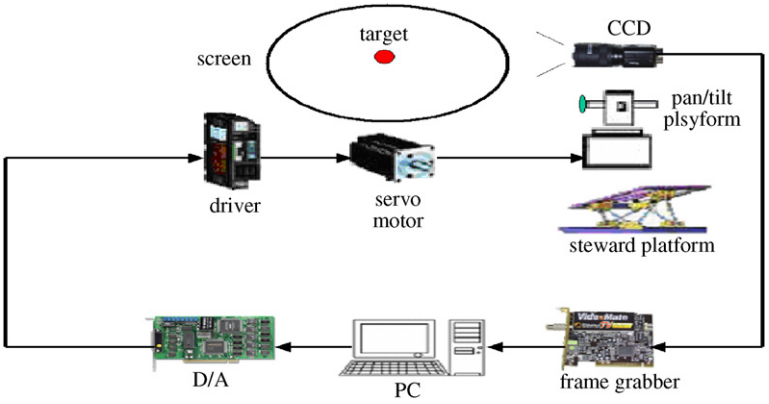

Fig. 4. The experimental setup.

Table 1
Single-axis vibration attenuation by ASC

	0.3 Hz	0.5 Hz	0.6 Hz	0.3 Hz + 0.5 Hz	0.4 Hz + 0.6 Hz
Yaw (dB)	27.31	24.55	24.51	23	21.55
Pitch (dB)	26.11	24.74	23.61	18.69	19.82

Table 2
Two-axis vibration attenuation by ASC

	0.3 Hz	0.5 Hz	0.6 Hz
Yaw (dB)	17.88	17.84	16.98
Pitch (dB)	20.98	16.96	16.88

Table 3
Single-axis vibration attenuation by feedback AVC

	0.3 Hz	0.5 Hz	0.6 Hz	0.3 Hz + 0.5 Hz	0.4 Hz + 0.6 Hz
Yaw (dB)	26.08	22.96	18.64	14.23	12.18
Pitch (dB)	26.33	21.87	22.05	13.17	11.35

Table 4
Two-axis vibration attenuation by feedback AVC

	0.3 Hz	0.5 Hz	0.6 Hz
Yaw (dB)	16.85	15.62	12.32
Pitch (dB)	16.78	13.87	15.61

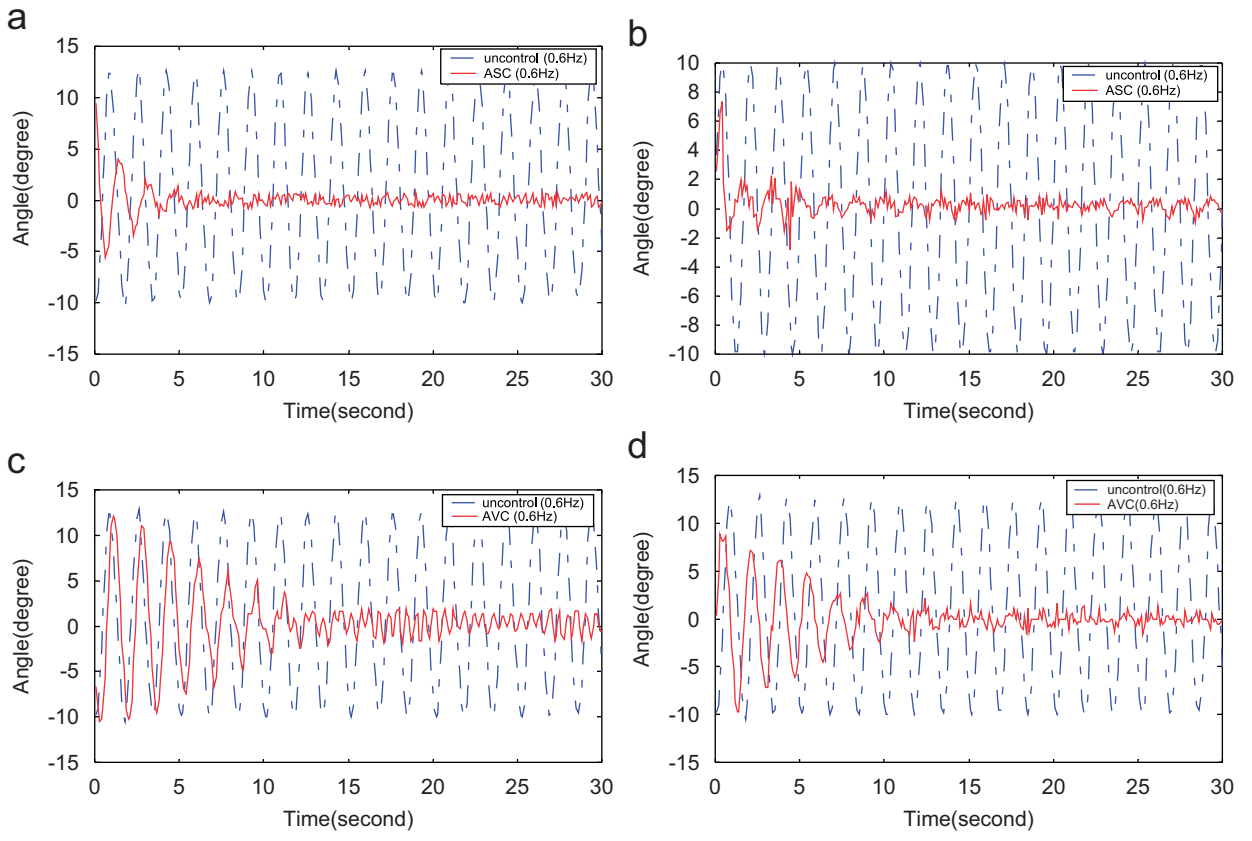

Fig. 5. Single axis vibration attenuation of 0.6 Hz sinusoidal disturbance: (a) ASC-yaw, (b) ASC-pitch, (c) AVC-yaw, (d) AVC-pitch.

3.3. Feedback AVC method

In this section, a feedback active vibration control method using adaptive filters is introduced [18]. Fig. 3 shows the corresponding block diagram of the method. In the block diagram, "plant" refers to the pan/tilt platform to be controlled. The control signal $u(t)$ from the controller and disturbance $d(t)$ from the Steward platform are the inputs to the plant, the resulting vibration response $y = \begin{bmatrix} x_1 & x_3 \end{bmatrix}^{\mathrm{T}}$ obtained also by a CCD camera is the variable to be minimized. The block marked "plant model" refers to the secondary path of the system, namely the dynamic from the control input $u(t)$ to system response $y(t)$. This block is needed for synthesizing the reference signal $x(t)$ for controller input and for filtering the reference signal $x(t)$ for obtaining $\bar{x}(t)$. In the experiment, the plant model and controller are to be modeled by an IIR and an FIR filter, namely by $s(n)$ and $w(n)$, respectively. In practice, off-line system identification method is used for constructing the IIR plant model $s(n)$ [19]. From identification experiment it is found that compared to the ASC, this control scheme needs two additional sensors of RVDT for inner loop servo motor position control using a simple proportional controller, since the plant model to be identified should be stable [18]. On the other hand, the FIR controller filter $w(n)$ is tuned on-line by the well-known filtered-x LMS method:

$$w(n+1) = w(n) + \eta \bar{x}(n) e(n), \tag{26}$$

$$\bar{x}(n) = s(n) x(n), \tag{27}$$

where $\bar{x}(n)$ in Eq. (27) is the filtered signal of $x(n)$ passing through the second path model $s(n)$ and η is a learning rate controlling the rate of convergence of the tuning algorithm.

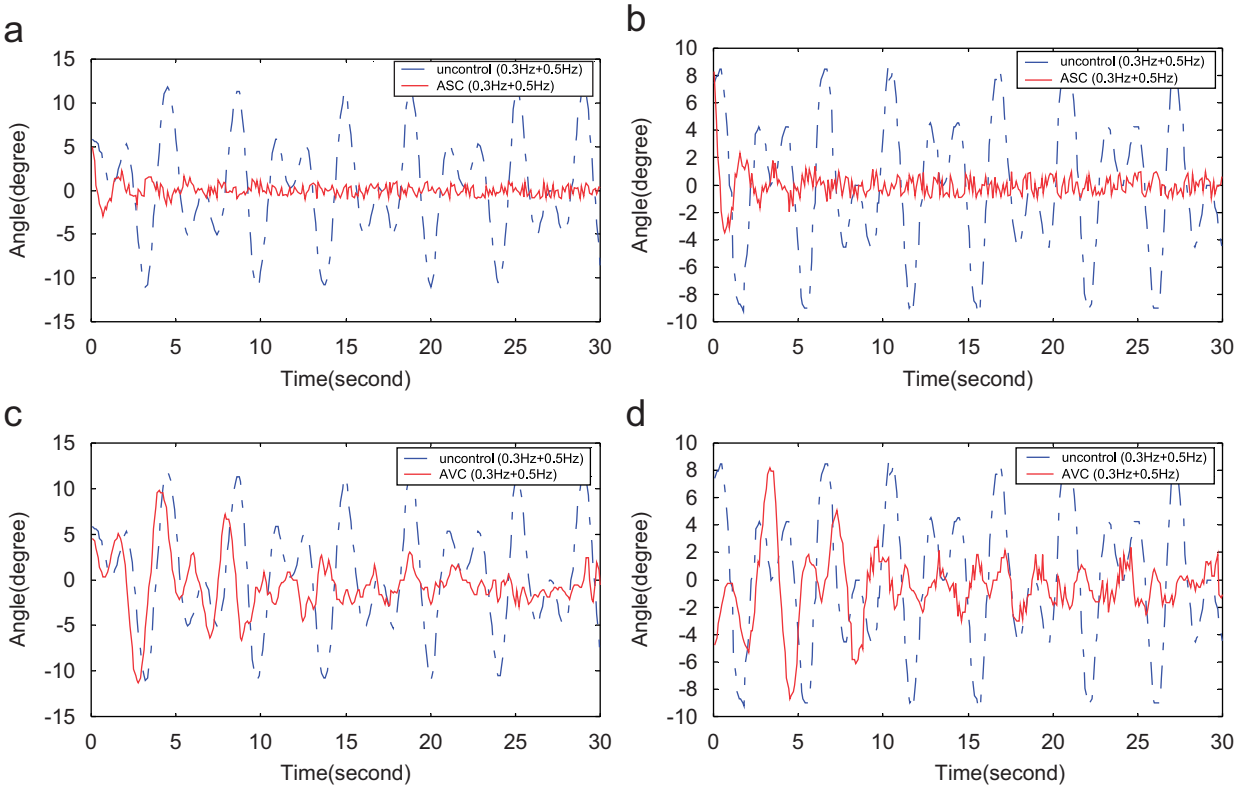

Fig. 6. Single axis vibration attenuation of 0.3 + 0.5 Hz sinusoidal disturbance: (a) ASC-yaw, (b) ASC-pitch, (c) AVC-yaw, (d) AVC-pitch.

4. Experimental results

In this section, an experimental setup is constructed to examine performance of the proposed controllers for yaw/pitch vibration suppression. The projected target point deviates from the center of the image plane due to base disturbance. Therefore, we need to drive the pan/tilt mechanism to bring the projected target back to the central point. The experimental setup is shown in Fig. 4. A fixed object (the so-called target) on a white screen, which is straightly ahead the pan/tilt platform, is captured by the CCD camera (see also Fig. 2(b)). Its image deviates from the origin in the image plane due to base disturbance. The deviation of the image can be calculated by the image processing algorithms described in Section 3.1. Control torques are computed by the proposed controllers based on these deviations and are supplied by servo motors to control the pan/tilt platform. A 12 bits D/A converter is used to interface with 1.8-GHz PC for sending out the control signals. The proposed control laws are programmed under Windows 2000 OS with 10 Hz sampling rate.

In the experiments, Steward platform provides three different low-frequency sinusoidal disturbances at 0.3, 0.5, and 0.6 Hz frequency to the pan/tilt platform base, in addition to the two-tone disturbances, 0.3 Hz + 0.5 Hz and 0.4 Hz + 0.6 Hz. A Fourier series with 15 finite terms is used to approximate these unknown disturbances. In this experiment, actual values of m_1 and m_2 are 2.132×10^3 and 7.91×10^4, respectively. The controller parameters of the ASC are chosen to be $\phi_k = 0.1$, $\eta_k = 10$ and $\lambda_k = 0.1$. For the feedback AVC method, we select an IIR filter for plant model, and an FIR filter for controller with learning rate $\eta = 0.0001$. The results of applying ASC and feedback AVC under above mentioned disturbances are summarized in Tables 1–4. It is noted that Tables 1 and 3 are for independent single axis excitations, while Tables 2 and 4 are for simultaneous two axes disturbances. Time responses of the vibration control of representative cases are shown in Figs. 5–7, where amplitudes can be clearly seen to diminish when controllers are activated. From theses experiment results, about 25.14 and 23 dB attenuations in average for

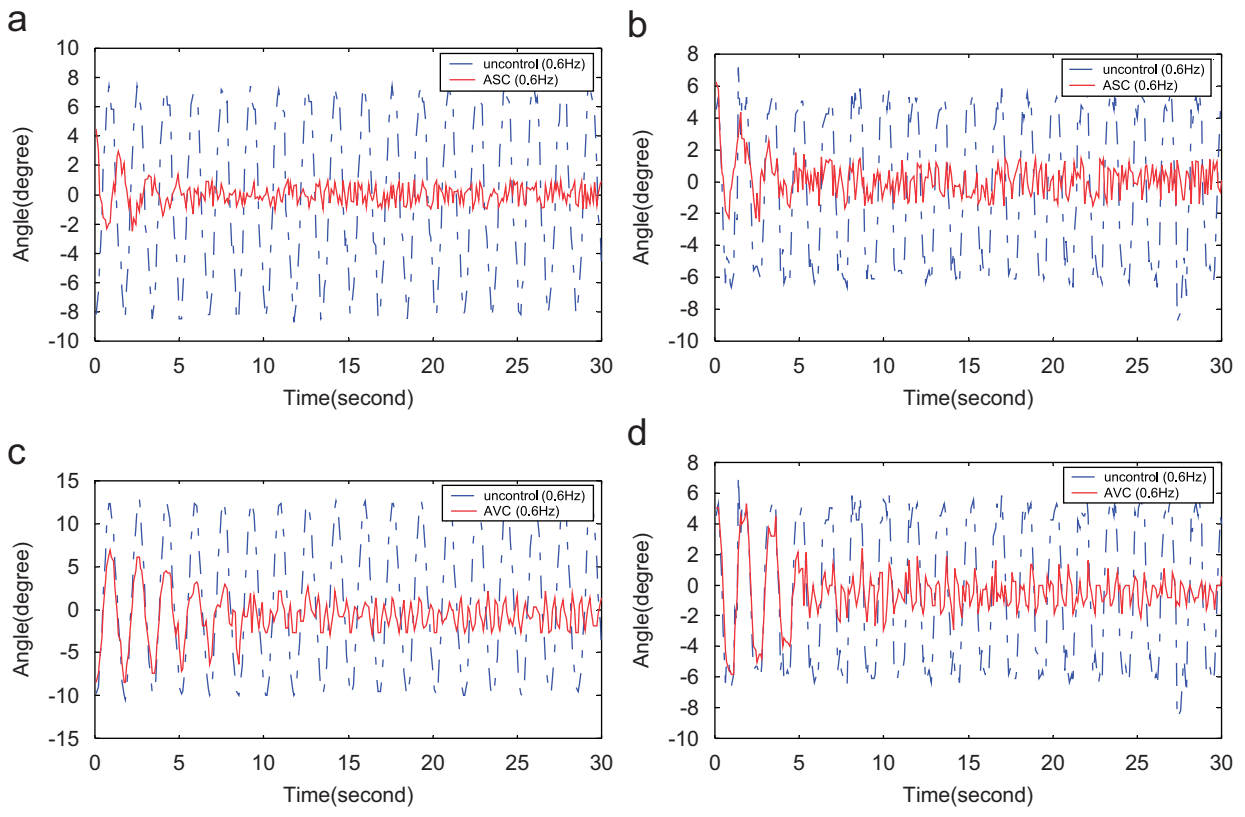

Fig. 7. Two axis vibration attenuation of 0.6 Hz sinusoidal disturbance: (a) ASC-yaw, (b) ASC-pitch, (c) AVC-yaw, (d) AVC-pitch.

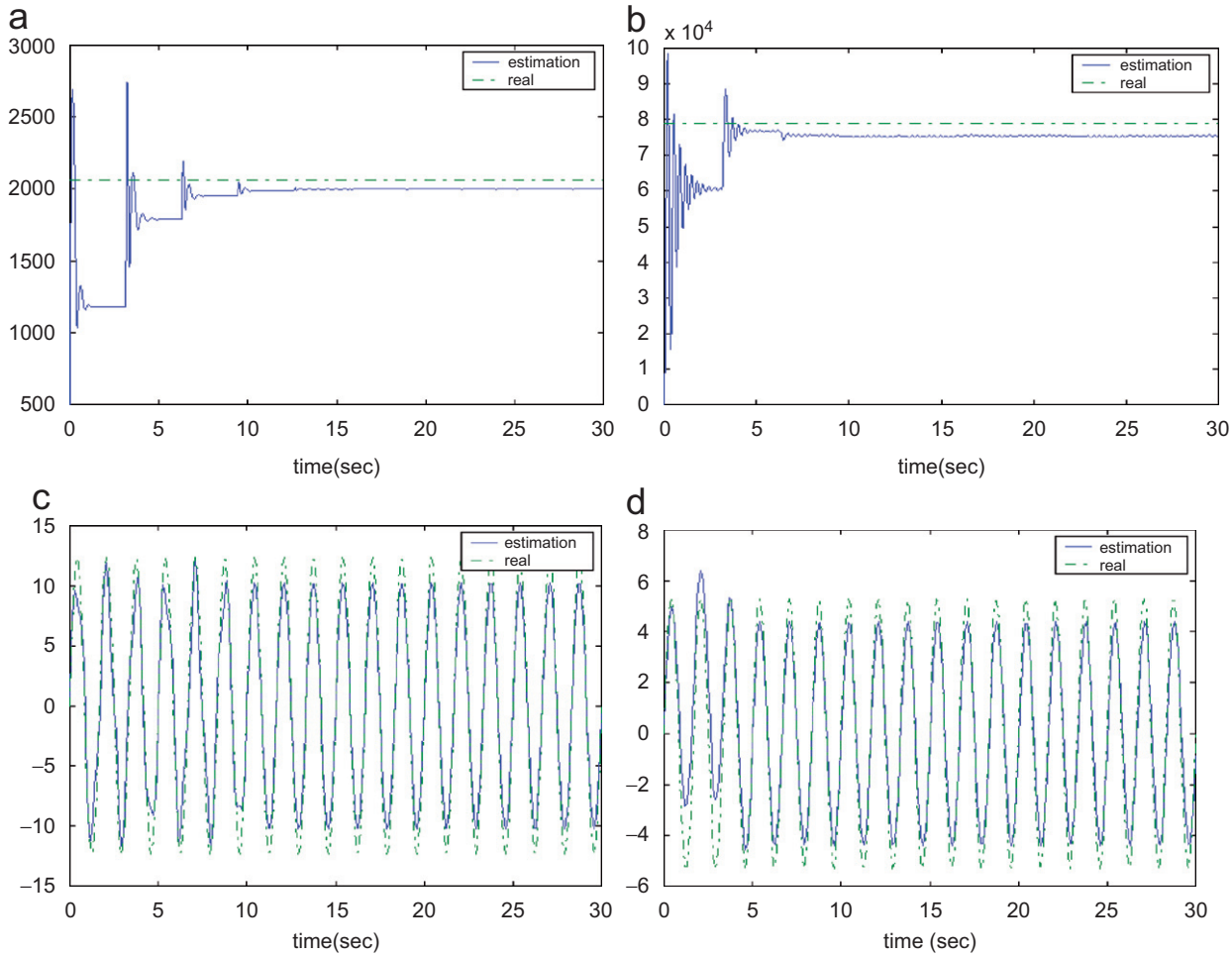

Fig. 8. Parameter estimations of two axis motion for 0.6 Hz disturbance: (a) estimation of m_1, (b) estimation of m_2, (c) estimation of d_1, (d) estimation of d_2.

single-frequency disturbance have been obtained by using the ASC and feedback AVC, respectively for independent single axis excitation. For dual-frequency excitation to each independent axis, the vibration attenuations are about 20.77 and 12.73 dB by the two methods, respectively. As for simultaneous two axes excitations, ASC and feedback AVC can achieve respective 17.57 and 15.18 dB vibration reductions under single-frequency disturbances. Fig. 8 shows results of parameter estimation when using ASC.

5. Conclusion

In this paper, adaptive sliding control and feedback AVC are used to deal with the time-varying disturbance and model uncertainty for vision feedback pan/tilt platform. The bound of disturbance in previous discussion is assumed to be unknown. The results in Section 4 indicate the vibration attenuation performance of the proposed control laws. Although the model parameter and disturbance bound are not available, we can still obtain good vibration attenuation.

The main object of function approximation is to transfer unknown function $d_k(t)$ into a linear combination of orthogonal basis so that the update law can be obtained by using Lyapunov stability theory. In Section 3.2, we have given a brief proof of the stability and update law. In this study, we can guarantee that the system output is asymptotical convergence. However, the estimation of m_k and $d_k(t)$ can only be proved that they are bounded. For all estimations to be convergent, the reference signal should be satisfying PE condition.

By the discussion in Section 3.3, we know that the feedback AVC method is effective to deal with vibration rejection. Even we do not have any information of the model and disturbance, this scheme still has ability to decrease the effect from disturbance, without using complex mathematics. Nevertheless, its transient response is poor as compared to that by the adaptive sliding control. From the time responses in Section 4, we find that the amplitude is hard to converge while the disturbance has more than one frequency component (see Figs. 6(c)–(d)). Moreover, the system convergence for stability is difficult to guarantee.

In this experiment, a fixed object in a simple background with white screen was used for target iamge feature acquiring. For the future work, problems with human face or moving target tracking in a more complex and realistic background and with pan/tilt platform disturbed will be studied.

Acknowledgments

This work was supported by National Science Council, Taiwan, under grant number NSC 93-2212-E-027-019.

References

[1] T. Inanc, A Novel Approach to Active Vision Systems: Modeling, Control and Real Time Tracking, PhD Thesis, Pennsylvania State University, 2002.
[2] M.E. Magana, F. Holzapfel, Fuzzy-logic control of an inverted pendulum with vision feedback, *IEEE Transactions on Education* 141 (2) (1998) 165–169.
[3] E.P. Dadios, R. Baylon, R. De Guzman, A. Florentino, R.M. Lee, Z. Zulueta, Vision guided ball-beam balancing system using fuzzy logic, *Proceedings of IECON 2000, 26th Annual Conference of the IEEE*, Vol. 3, October 2000, pp. 1973–1978.
[4] P.I. Corke, M.C. Good, Dynamic effects in visual closed-loop systems, *IEEE Transactions on Robotics and Automation* 12 (5) (1996) 671–683.
[5] K. Hashimoto, T. Ebine, H. Kimura, Visual servoing with hand-eye manipulator-optimal control approach, *IEEE Transactions on Robotics and Automation* 12 (5) (1996) 766–774.
[6] N.P. Papankolopoulos, P.K. Khosla, Adaptive robotic visual tracking: theory and experiment, *IEEE Transactions on Automatic Control* 38 (3) (1993) 429–445.
[7] D.Y. Jeong, J. Lee, Y.K. Kim, A study on camera tracking system using a self-tuning regulator in visual feedback control, *Proceedings. ISIE 2001, IEEE International Symposium*, Vol. 3, June 2001, pp. 1591–1596.
[8] J.E. Slotine, W. Li, *Applied Nonlinear Control*, Prentice-Hall, Englewood Cliffs, NJ, 1991.
[9] A.C. Huang, Y.S. Kuo, Sliding control of nonlinear systems containing time-varying uncertainties with unknown bounds, *International Journal of Control* 74 (3) (2001) 252–264.
[10] M.C. Chien, A.C. Huang, Adaptive impedance control of robot manipulators based on function approximation technique, *Robotica* 22 (2004) 395–403.
[11] A.C. Huang, Y.C. Chen, Adaptive sliding control for single-link flexible-joint robot with mismatched uncertainties, *IEEE Transactions on Control Systems Technology* 12 (5) (2004) 770–775.
[12] A.C. Huang, Y.C. Chen, Adaptive multiple-surface sliding control for non-autonomous systems with mismatched uncertainties, *Automatica* 11 (40) (2004) 1939–1945.
[13] P.C. Chen, A.C. Huang, Adaptive multiple-surface sliding control of hydraulic active suspension systems based on the function approximation technique, *Journal of Vibration and Control* 11 (5) (2005) 685–706.
[14] A.C. Huang, S.C. Wu, W.F. Ting, A FAT-based adaptive controller for robot manipulators without regressor matrix: theory and experiments, *Robotica* 24 (2006) 205–210.
[15] D. Steward, A platform with six degrees of freedom, *Proceedings of the Institution of Mechanical Engineers* 180 (1 and 5) (1965) 371–386.
[16] R.C. Gonzalez, R.E. Woods, *Digital Image Processing*, Prentice-Hall, Englewood Cliffs, NJ, 2002.
[17] J.T. Spooner, M. Maggiore, R. Ordonez, K.M. Passino, *Stable Adaptive Control and Estimation for Nonlinear Systems-Neural and fuzzy Approximation Techniques*, Wiley, New York, 2002.
[18] S.M. Kuo, D. Morgan, *Active Noise Control Systems*, Wiley, New York, 1996.
[19] J. Shaw, Hybrid control of a cantilevered ER sandwich beam for vibration suppression, *Journal of Intelligent Material Systems and Structures* 11 (1) (2000) 26–31.